

## Mechanism of BINOL–Phosphoric Acid-Catalyzed Strecker Reaction of Benzyl Imines

Luis Simón and Jonathan M. Goodman\*

Unilever Centre For Molecular Science Informatics, Department of Chemistry, Lensfield Road, Cambridge, CB2 1EW, U.K.

Received November 10, 2008; E-mail: jmg11@cam.ac.uk

**Abstract:** The mechanism and the origin of the selectivity for the BINOL–phosphoric acid-catalyzed Strecker reaction on N-benzyl imines has been investigated by theoretical methods and compared with earlier studies of N-aryl imines. ONIOM calculations show that the reverse in selectivity which is observed experimentally is not due to differences in the steric bulk of aryl and benzyl groups, but rather because of a switch from a preference for a *Z* imine to an *E* imine in the transition state of benzaldehyde-derived imines. The calculations predict this change will not be present for imines formed from acetophenone.

### Introduction

Chiral BINOL–phosphoric acid derivatives<sup>1,2</sup> are very useful catalysts for the addition of nucleophiles to aryl<sup>3–16</sup> and acyl<sup>17–28</sup> imines. In order for these reactions to have synthetic applications, it is important that cleavage of the N-substituent

can be performed under mild conditions and with high yields. This is the case for *p*-methoxy aryl imines, for which the cleavage reaction can be performed under oxidizing conditions.<sup>29</sup> If these reactions could be applied to *p*-methoxybenzyl imines, the synthetic applicability would be further increased, since this group can also be cleaved using very mild reduction conditions.<sup>30</sup> Examples of enantioselective Strecker reactions of this and other benzyl imines are scarce. List has shown that a thiourea-based catalyst works well for acylcyanation of benzyl imines, but that BINOL–phosphoric acid catalysts are less effective.<sup>31</sup> Rueping<sup>32,33</sup> has demonstrated that BINOL–phosphoric acid catalysts are useful for the addition of HCN to benzyl imines (the Strecker reaction<sup>34</sup>).

In our study of the mechanism of Hantzsch ester hydrogenation of aryl-imines, we proposed a model to explain the enantioselectivity of the reaction of aryl-imines (Figure 1).<sup>35</sup> This model was based on the presence of simultaneous stabilizing interactions of the catalyst with the nucleophile and electrophile and with the different steric interactions with the competing diastereomeric transition states, adapting the classical

- (1) Akiyama, T. *Chem. Rev.* **2007**, *107*, 5744–5758.
- (2) (a) Brunel, J. M. *Chem. Rev.* **2005**, *105*, 857–898. (b) Brunel, J. M. *Chem. Rev.* **2007**, *107*, PR1–PR45.
- (3) Guo, Q.-S.; Du, D.-M.; Xu, J. *Angew. Chem., Int. Ed.* **2008**, *47*, 759–762.
- (4) Hoffmann, S.; Seayad, A. M.; List, B. *Angew. Chem., Int. Ed.* **2005**, *44*, 7424–7427.
- (5) Rueping, M.; Antonchick, A. P.; Brinkmann, C. *Angew. Chem., Int. Ed.* **2007**, *46*, 6903–6906.
- (6) Rueping, M.; Antonchick, A. P.; Theissmann, T. *Angew. Chem., Int. Ed.* **2006**, *45*, 6751–6755.
- (7) Guo, Q.-X.; Liu, H.; Guo, C.; Luo, S.-W.; Gu, Y.; Gong, L.-Z. *J. Am. Chem. Soc.* **2007**, *129*, 3790–3791.
- (8) Hoffmann, S.; Nicoletti, M.; List, B. *J. Am. Chem. Soc.* **2006**, *128*, 13074–13075.
- (9) Li, G.; Liang, Y.; Antilla, J. C. *J. Am. Chem. Soc.* **2007**, *129*, 5830–5831.
- (10) Storer, R. I.; Carrera, D. E.; Ni, Y.; MacMillan, D. W. C. *J. Am. Chem. Soc.* **2006**, *128*, 84–86.
- (11) Zhou, J.; List, B. *J. Am. Chem. Soc.* **2007**, *129*, 7498–7499.
- (12) Akagawa, K.; Akabane, H.; Sakamoto, S.; Kudo, K. *Org. Lett.* **2008**, *xx*.
- (13) Akiyama, T.; Morita, H.; Itoh, J.; Fuchibe, K. *Org. Lett.* **2005**, *7*, 2583–2585.
- (14) Liu, H.; Cun, L.-F.; Mi, A.-Q.; Jiang, Y.-Z.; Gong, L.-Z. *Org. Lett.* **2006**, *8*, 6023–6026.
- (15) Rueping, M.; Sugiono, E.; Azap, C.; Theissmann, T.; Bolte, M. *Org. Lett.* **2005**, *7*, 3781–3783.
- (16) Kang, Q.; Zhao, Z.-A.; You, S.-L. *Adv. Synth. Catal.* **2007**, *349*, 1657–1660.
- (17) Terada, M.; Yokoyama, S.; Sorimachi, K.; Uruguchi, D. *Adv. Synth. Catal.* **2007**, *349*, 1863–1867.
- (18) Jia, Y.-X.; Zhong, J.; Zhu, S.-F.; Zhang, C.-M.; Zhou, Q.-L. *Angew. Chem., Int. Ed.* **2007**, *46*, 5565–5567.
- (19) Rueping, M.; Antonchick, A. P.; Theissmann, T. *Angew. Chem., Int. Ed.* **2006**, *45*, 3683–3686.
- (20) Terada, M.; Machioka, K.; Sorimachi, K. *Angew. Chem., Int. Ed.* **2006**, *45*, 2254–2257.
- (21) Terada, M.; Soga, K.; Momiyama, N. *Angew. Chem., Int. Ed.* **2008**, *47*, 4122–4125.
- (22) Kang, Q.; Zheng, X.-J.; You, S.-L. *Chem.-Eur. J.* **2008**, *14*, 3539–3542.

- (23) Qiang Kang, Q.; Zhao, Z.-A.; You, S.-L. *J. Am. Chem. Soc.* **2007**, *129*, 1484–1485.
- (24) Terada, M.; Machioka, K.; Sorimachi, K. *J. Am. Chem. Soc.* **2007**, *129*, 10336–10337.
- (25) Terada, M.; Sorimachi, K. *J. Am. Chem. Soc.* **2007**, *129*, 292–293.
- (26) Uruguchi, D.; Terada, M. *J. Am. Chem. Soc.* **2004**, *126*, 5356–5357.
- (27) Li, G.; Rowland, G. B.; Rowland, E. B.; Antilla, J. C. *Org. Lett.* **2007**, *9*, 4065–4068.
- (28) Li, G.; Fronczek, F. R.; Antilla, J. C. *J. Am. Chem. Soc.* **2008**, *130*, 12216–12217.
- (29) Verkade, J. M. M.; van Hemert, L. J. C.; Quaedflieg, P. J. L. M.; Alsters, P. L.; van Delft, F. L.; Rutjes, F. P. J. T. *Tetrahedron Lett.* **2006**, *47*, 8109–8113.
- (30) Gatto, V. J.; Miller, S. R.; Gokel, G. W.; Prabhakaran, P. C.; White, J. D. *Org. Synth.* **1990**, *68*, 227–230.
- (31) Pan, S. C.; Zhou, J.; List, B. *Angew. Chem., Int. Ed.* **2007**, *46*, 612–614.
- (32) Rueping, M.; Sugiono, E.; Azap, C. *Angew. Chem., Int. Ed.* **2006**, *45*, 2617–2619.
- (33) Rueping, M.; Sugiono, E.; Moreth, S. A. *Adv. Synth. Catal.* **2007**, *349*, 759–764.
- (34) Strecker, A. *Ann. Chem. Pharm.* **1850**, *75*, 27–45.
- (35) Simón, L.; Goodman, J. M. *J. Am. Chem. Soc.* **2008**, *130*, 8741–8747.

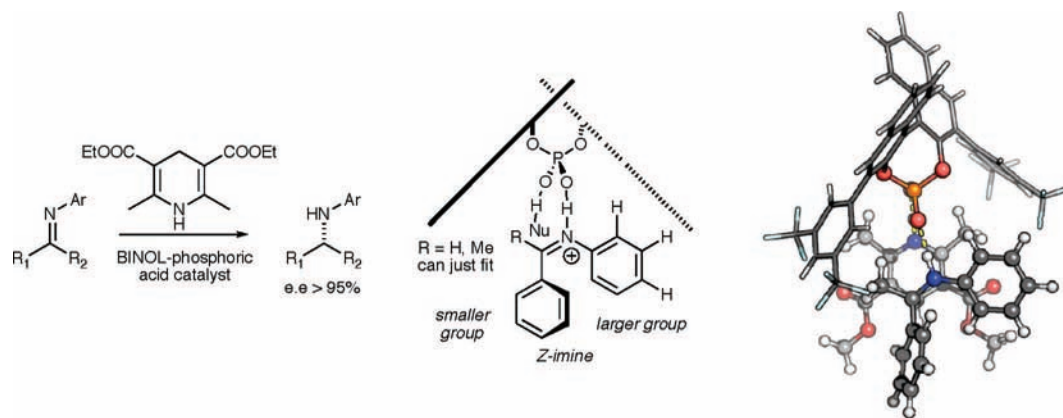


**Figure 1.** Enantioselectivity in the Hantzsch ester hydrogenation of aryl-imines.<sup>35</sup>

“three point interaction model”.<sup>36</sup> Akiyama has proposed this type of mechanism for the addition of hydrophosphonylation of imines<sup>37a</sup> and more recently for the Friedel–Crafts reaction of indoles with nitroalkenes.<sup>37b</sup> This is also the preferred mechanism in Terada’s recent review,<sup>37c</sup> and Himo has reached similar conclusions independently.<sup>38</sup> A similar analysis can also be used to explain the enantioselectivity of alkenylboronate additions to enones catalyzed by substituted binaphthols.<sup>39</sup>

The success of these analyses lead us to consider whether a similar model could be applied to the Strecker reaction, despite the differences between the systems. The model in Figure 1 fits the Strecker reaction if the nucleophile (NuH) is changed from the Hantzsch ester to HCN, and the imine from a N-phenyl imine to a N-benzyl imine with R = H. Rueping’s experimental studies, however, showed that the major product had S configuration,<sup>32</sup> the opposite to that found for attack on N-aryl imines (Scheme 2). One possible explanation is that the benzyl group’s flexibility makes it smaller than the aryl group, and so the major interactions are reversed. However, it is also possible that the E-imine rather than the Z-imine is on the lowest energy pathway for these systems, or that some different effect leads to the change. Rueping also reports that the reaction gives good enantioselectivity with an acetophenone-based imine (R = Me, Figure 1).<sup>33</sup> In these examples the absolute stereochemistry of the products was not reported. A computational analysis should be able to predict the product stereochemistry of this reaction.

In this paper, we report calculations on the mechanism of the Strecker reaction on N-benzyl imines, with the aim of identifying the factors that control the enantioselectivity and testing whether the model can predict the enantioselectivity of BINOL–phosphoric-catalyzed reactions for these useful substrates. We start with the study of different possible reaction mechanisms with a simplified catalyst model, and the lowest energy pathways are then used to study the enantioselectivity when chiral ligands are included. We use these results to suggest a model for the enantioselectivity of the Strecker reaction and to predict the likely stereochemical outcome of the acetophenone-based reaction.

**Reaction Pathway Simplified Catalyst Structure.** We have performed a DFT analysis of the Strecker reaction on N-benzyl imine of acetophenone (Figure 2) catalyzed by buta-1,3-diene-1,4-diol-phosphoric acid, a model for the phosphoric acid catalyst. We compared four different pathways, and the results are illustrated in Figure 2, along with Gibbs free energy barriers (relative in all cases to the most stable complex between the imine and the catalyst and to hydrogen cyanide). Transition structures in which the catalyst establishes interactions only with HCN were included in the study (TS-1E and TS-1Z). However, lower energies were found for all the other transition structures in which the catalyst interacts with both the HCN molecule and the imine. This double interaction has been crucial for explaining the enantioselectivity of the reactions of N-aryl-imines,<sup>35</sup> and so should also be of relevance for understanding N-benzyl-imine reactions. These results are consistent with the preferred pathway from Han’s recent DFT study of the mechanism of the Strecker reaction catalyzed by guanidines.<sup>40</sup>

TS-2E and TS-2Z (Figure 2) show the reaction with hydrogen cyanide to form an alkyl isocyanide product that can isomerize to yield the product of the reaction.<sup>40</sup> This route is slightly more favorable than the singly coordinated possibilities (TS-1E and TS-1Z) but still passes through high-energy transition states. Since TS-2E and TS-2Z are so high in energy, this path is unfavorable, whatever the energy barrier for the isomerization of the isocyanide product.

The lowest energy transition states are obtained when the nucleophile is hydrogen isocyanide (TS-3E and TS-3Z) rather than hydrogen cyanide, even though hydrogen isocyanide has a higher energy by 13.4 kcal/mol than hydrogen cyanide. We have calculated the activation free energy,  $\Delta G^\ddagger$ , for the isomerization of the hydrogen cyanide is 23.5 kcal/mol, when this reaction is catalyzed by the phosphoric acid catalyst. Amines generated in the reaction might also aid this process. The energy barrier for the isomerization mediated by ammonia is 19.9 kcal/mol (see Supporting Information). This isomerization, therefore, has an activation barrier smaller than any of the reactions involving the hydrogen cyanide. This shows that the isomerization is a fast process, compared with the direct reaction of hydrogen cyanide with the imine. The possibility of hydrogen cyanide attacking through its carbon atom rather than its nitrogen atom was also considered (TS4-E; attempts to find an analogous TS4-Z always lead to the TS-3Z structure). This transition structure is higher in energy than both TS-3E and TS-3Z. The

(36) Easson, L. H.; Stedman, E. *J. Biochem.* **1933**, *27*, 1257–1266.

(37) (a) Akiyama, T.; Morita, H.; Itoh, J.; Fuchibe, K. *Org. Lett.* **2005**, *7*, 2583–2585. (b) Itoh, J.; Fuchibe, K.; Akiyama, T. *Angew. Chem., Int. Ed.* **2008**, *47*, 4016–4018. (c) Terada, N. *Chem. Commun.* **2008**, 4097–4112.

(38) Marcelli, T.; Hammar, P.; Himo, F. *Chem.-Eur. J.* **2008**, *14*, 8562–8571.

(39) Paton, R. S.; Goodman, J. M.; Pellegrinet, S. C. *J. Org. Chem.* **2008**, *73*, 5078–5089.

(40) Li, J.; Jiang, W.-Y.; Han, K.-L.; He, G.-Z.; Li, C. *J. Org. Chem.* **2003**, *68*, 8786–8789.

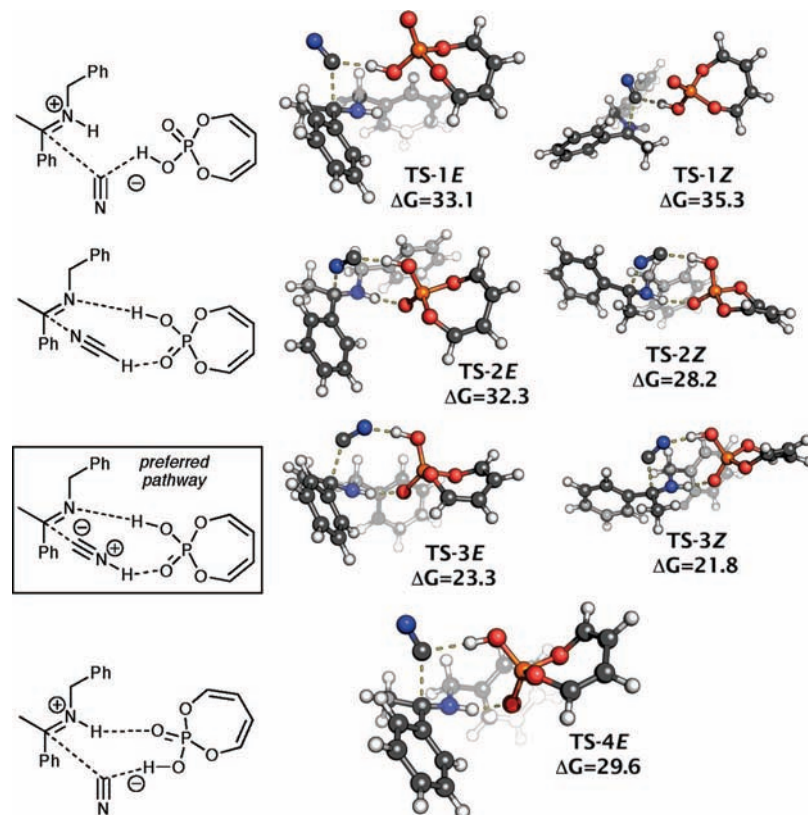


**Figure 2.** Transition states found for the reaction of acetophenone-derived N-benzylimine using a simplified model of the catalyst. Gibbs free energies are expressed in kcal/mol.

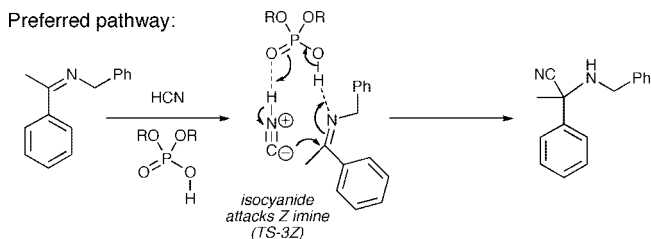


**Figure 3.** Preferred pathway: attack of an isocyanide on a Z acetophenone-derived imine.

best pathway for the reaction is, therefore, through doubly coordinated hydrogen isocyanide (TS-3E and TS-3Z), Figure 3.

The relative energy of transition states following from Z and from E imines is very important in determining the absolute configuration of the product. Under the reaction conditions, substrate isomerization from the E to the Z imine is possible. The barrier height for this kind of isomerization is high,<sup>41,42</sup> but equilibration has been found, even at low temperatures, if hydroxyl groups are present.<sup>43,44</sup> Therefore, the reaction will proceed through the lower energy transition state, even if this does not correspond to the thermodynamically preferred isomer of the starting material. Like the reaction of Hantzsch ester with the N-phenyl imine derived from acetophenone,<sup>35</sup> the Z transi-

tion states are more stable. The difference in energy between TS-3Z and TS-3E is only 1.5 kcal/mol, rather less than the corresponding difference for the Hantzsch ester reduction. Similar transition states for the Strecker reaction on N-phenyl imine derived from acetophenone have a 2.6 kcal/mol energy difference, showing that the Z transition states are more favored for aryl imines than for benzyl imines. If acetophenone is replaced by benzaldehyde, however, the ground-state preference for the E form greatly increases. The N-benzyl imine derived from benzaldehyde has lower energy transition structures for the E form than the Z form. This contrasts with the behavior of the N-phenyl imine derived from benzaldehyde for which the Z transition structures are more stable by 1.1 kcal/mol, despite the thermodynamic preference for the E form in the ground state of the imine.

**Stereoselectivity Full Catalyst Structure.** These DFT calculations showed that the best pathway for the reaction is though the attack of isocyanide (TS-3E and TS-3Z) on the N-benzyl imine. The Z imine geometry is preferred for acetophenone-derived imines, and the E imine geometry is preferred for benzaldehyde-derived imines. In order to explain the enantioselectivity of the 9-phenanthrene BINOL-phosphoric acid catalyzed reaction (Scheme 1), ONIOM calculations were performed. These calculations make it possible to study systems as large as the chiral ligands in these reactions and also allow us to quantify steric interactions between the ligands and the reacting centers. An exhaustive survey of possible transition states was done, scanning over E and Z configurations of the imine and different conformations of the benzyl group and of the two 9-phenanthrene groups in the catalyst. Overall, 40 transition structures were located for each substrate. Despite of the flexibility of the phenanthrene groups, dihedral angle

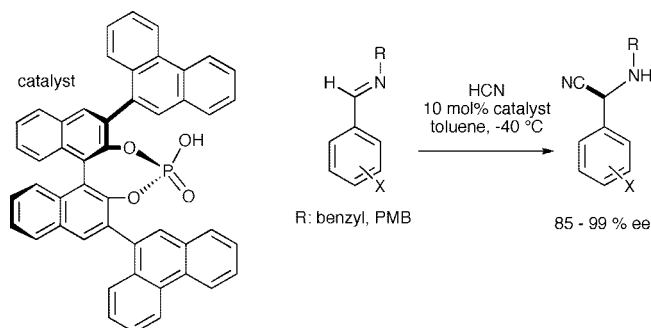
(41) Banik, B. K.; Lecea, B.; Arrieta, A.; de Cózar, A.; Cossío, F. P. *Angew. Chem., Int. Ed.* **2007**, *46*, 9347–9438.

(42) Tommaso Marcelli, F. H. *Eur. J. Org. Chem.* **2008**, *2008*, 4751–4754.

(43) Berthet, J.; Delbaere, S.; Carvalho, L. M.; Vermeersch, G.; Coelho, P. J. *Tetrahedron Lett.* **2006**, *47*, 4903–4905.

(44) Traven, V. F.; Miroshnikov, V. S.; Pavlov, A. S.; Ivanov, I. V.; Panov, A. V.; Chibisova, T. y. A. *Mendeleev Commun.* **2007**, *17*, 88–89.



**Scheme 1.** Rueping's Highly Enantioselective Chiral BINOL–Phosphoric Acid-Catalysed Strecker Reaction<sup>32</sup>

between the two naphthyl rings in BINOL moiety is quite constant, around  $65^\circ \pm 2^\circ$ . Zero-point energies of all these structures were used to calculate their contributions to each product enantiomer, using a Boltzmann distribution.

In agreement with the results of the DFT calculations on the simplified catalyst, the major pathway is through the *E* imine for acetophenone-derived *N*-benzylimines. For the reaction of benzaldehyde-derived *N*-benzylimine, 86% ee of the *S* product is calculated, in excellent agreement with experimental results (85–97% ee, depending on the substituents on aromatic rings<sup>32</sup>).

The lowest energy transition structures were examined to identify the origin of the enantioselectivities for benzaldehyde-derived imines. The lowest energy transition structure, which leads to the *S* product (TS-5E-S) and the two lowest energy transition structures leading to *R* product (TS-5E-R, zpE: +1.4 kcal/mol, and TS-5E-R', zpE: 1.7 kcal/mol) were chosen (Figure 4).<sup>45</sup> All these structures have the *E* conformation of the imine. The ONIOM calculations suggest that the steric interactions in the transition structure stabilize TS-5E-R with respect to TS-5E-S, but the energy required to twist the substrate into the necessary conformation for this transition structure more than compensates for the steric effects. TS-5E-R' has a similar conformation to TS-5E-S, but steric effects, in particular between the benzyl group and the closer phenanthryl ring, lead to the higher energy.

For the acetophenone-derived imine, a larger number of transition structures contribute significantly to the product distribution (Figure 5). The most stable transition state (TS-6Z-R) corresponds to a *Z* imine conformation and yields the *R* product. Another *Z* transition state (TS-6Z-S,  $\Delta\Delta$ zpE: +0.9 kcal/mol), yielding the *S* product, has a higher energy. TS-6E-R ( $\Delta\Delta$ zpE: +0.7 kcal/mol) and TS-6E-S ( $\Delta\Delta$ zpE: +0.9 kcal/mol), with *E* imine conformation, are (overall) destabilized as a consequence of steric interactions between the phenanthrene rings in chiral catalyst and the reacting species ((3.7) + (−2.9) = 0.8 kcal/mol for TS-6E-R and (+3.5) + (−2.1) = 1.4 kcal/mol for TS-6E-S). The lower stability of TS-6E-R' and TS-6E-S' is a consequence of the higher energy of the conformation of the atoms involved with bond forming and bond breaking processes in these transition structures. In TS-6E-S', steric effects with the phenanthrene rings are more favorable than in the other structures, even though the benzyl aromatic ring is oriented toward one of the aromatic sheets of the binaphthyl group.

(45) A fourth transition state leading to the *S* product was not included despite showing a zero-point energy only 0.9 kcal/mol higher than TS-5E-S. Its structure differs only in the conformation of a phenanthrene ring to that of TS-5E-S, and therefore, the factors which determine the TS-5E-S stability will also control this structure. The remaining transition structures have energies more than 3.0 kcal/mol above TS-5E-S.

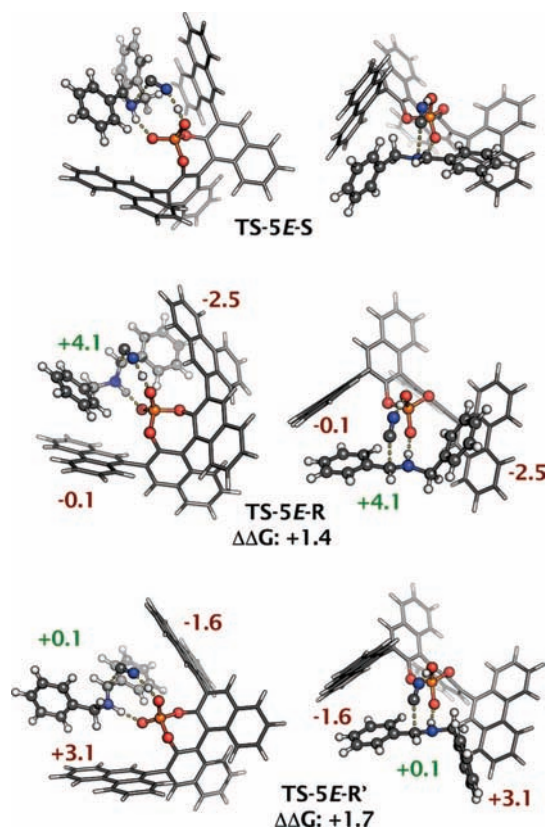


**Figure 4.** Transition states found for the reaction of *N*-benzylimine derived from benzaldehyde. Two views of each structure are shown. In both, the cyanide is at the front. On the left, the BINOL group is at the lower right-hand corner; on the right, the BINOL group is at the back. Zero-point energies are expressed in kcal/mol. Steric interactions (in red) and conformation effects (green), relative to analogous effects in TS-5E-S are also expressed in kcal/mol (see Computational Details). All the pathways through the *Z* imines are higher in energy for these benzaldehyde-derived imines.

At the temperature of the experiment (233 K) an energy difference of 0.7 kcal/mol corresponds to an ee of about 55%. Taking account of all 40 competing transition structures for the acetophenone-derived imine, the calculations suggest that the *R* product should be formed in 58% ee. The experimental results are 56–80% ee and the absolute configuration of the major enantiomer obtained is not reported.<sup>33</sup> We can, therefore, predict that the major enantiomer will be *R*, the opposite configuration to that obtained for the corresponding benzaldehyde-derived reaction. In this case, the *Z* imine geometry is on the preferred pathway.

## Discussion

The reverse in selectivity shown in Scheme 2 could be explained either by a change from the *Z* to the *E* imine on the most favorable reaction pathways, or else by a benzyl group being much less sterically demanding than an aryl group, because of its greater conformational flexibility. Our calculations show that the reverse in selectivity is due to a change from a *Z*-imine pathway to an *E*-imine pathway. The benzyl group, like the aryl group takes up the most sterically demanding position in the transition state.

**Imine *Z/E* Conformation.** For benzaldehyde-derived imines, the *N*-phenyl imine *Z* transition structure is 1.1 kcal/mol more stable than the *N*-phenyl *E* one. However, for *N*-benzyl imine, the *E* transition structure is 2.9 kcal/mol more stable. Therefore,

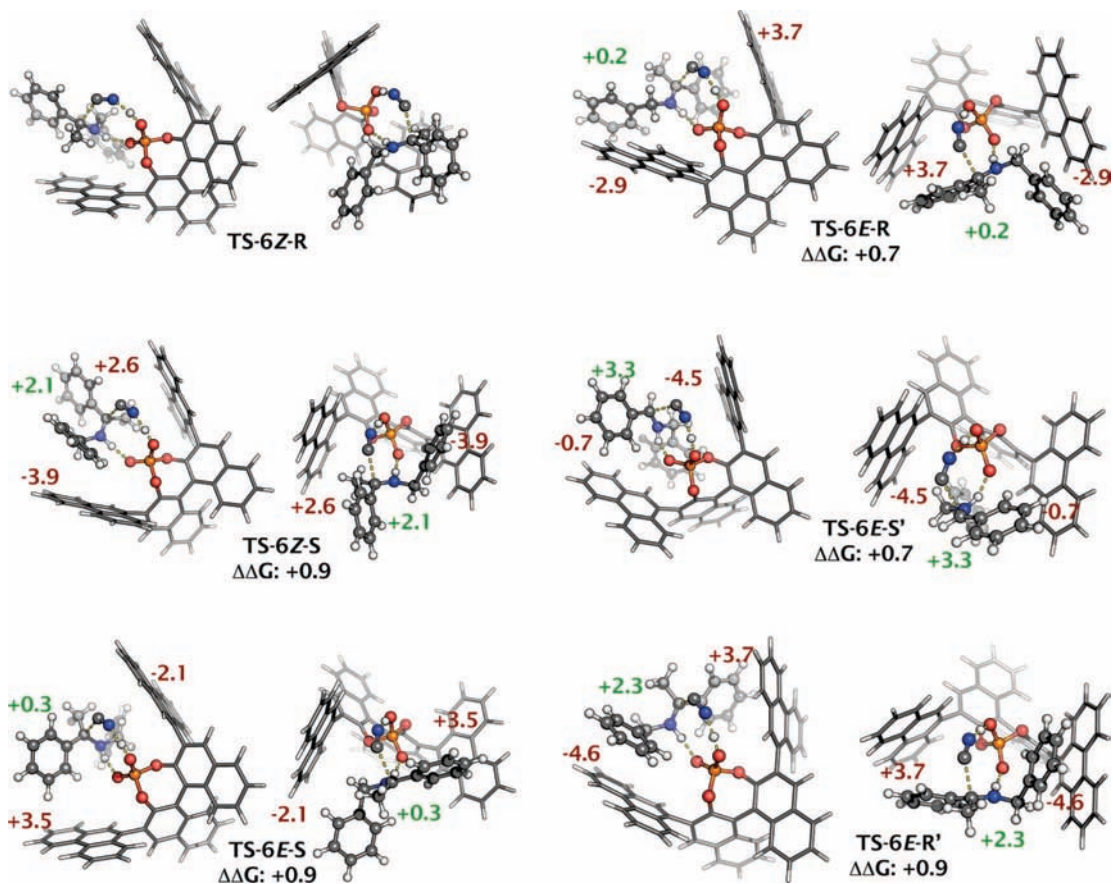
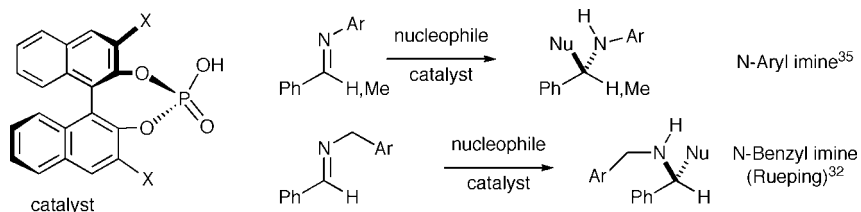


**Figure 5.** Transition states found for the reaction of *N*-benzyl imine derived from acetophenone. Two views of each structure are shown. In both, the cyanide is at the front. On the left, the BINOL group is at the lower right-hand corner; on the right, the BINOL group is at the back. Energies are expressed in kcal/mol. Steric and conformation effects are relative to analogous effects in TS-6Z-S (see Supporting Information).

**Scheme 2.** Comparison of the Reactions of Aryl and Benzyl Imines with Nucleophiles



*N*-benzyl *Z* transition structures do not contribute significantly to the product, and for the *N*-benzyl imine the enantioselectivity should be reversed and higher than for the *N*-phenyl imine. A practical consequence is that *p*-methoxybenzyl substitution should lead to higher enantioselectivities than *p*-methoxyphenyl substitution in the reactions of aldehyde-derived imines. This agrees with reports of relatively low selectivities for the reactions of *N*-(*p*-methoxyphenyl)-benzaldehyde imine derivatives (e.g., 52% ee for hydrophosponylation,<sup>13</sup> or 80:20–85:15 diastereomeric ratios in a hetero Diels–Alder reaction<sup>14</sup> or in Mannich reaction of cyclohexenone<sup>14</sup>).

For the acetophenone-derived *N*-benzyl imine, *Z* transition structures are more stable than *E* transition structures, but the difference is reduced with respect to the reaction of acetophenone-derived *N*-phenyl imine. This implies that enantioselectivity should be reduced since the *N*-benzyl *Z* and *N*-benzyl *E* geometries lead to different enantiomers of the product. This is consistent with the experimental data: *N*-(*p*-methoxybenzyl)-benzaldehyde-derived imines give higher enantioselectivities than acetophenone-derived imines.<sup>32,33</sup>

**Interactions with the Chiral Catalyst.** Because benzyl groups are conformationally flexible, it might be expected that they should be sterically less demanding than aryl groups. This is inconsistent with both experimental and computational results for the Strecker reaction of imines. Benzyl groups must be sufficiently sterically demanding to prefer the least hindered positions in the transition states of these reactions.

A part of the explanation for this is that the barriers for the rotation of benzyl groups are fairly large. The conformational preferences and barriers for the *N*-benzyl group were investigated using relaxed scan calculations around the C=N–C–C dihedral angle for the transition state from the different iminium substrates. These reveal that the more stable transition states correspond to the more stable rotamers of the substrate (Figure 6). The C=N–C–C dihedral angle in TS-6E-S' corresponds to a substrate structure destabilized by 1 kcal/mol. The estimated conformational destabilization in this transition state (3.3 kcal/mol) includes also the lower stability of *E* transition states for this substrate.



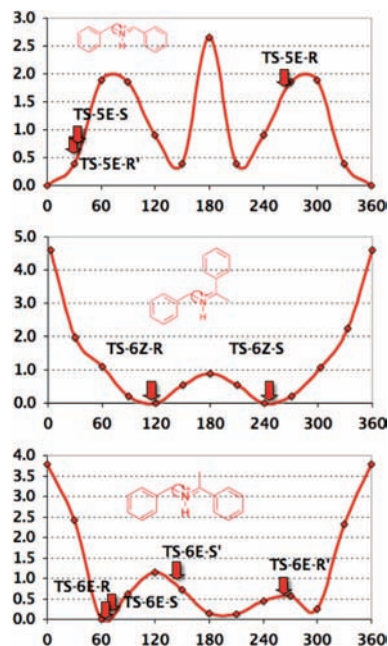


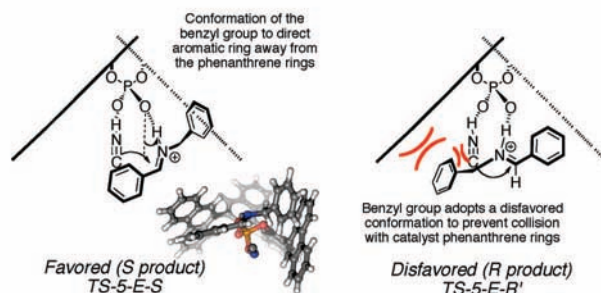
**Figure 6.** Relaxed scan calculation on the  $C=N-C-C$  dihedral angle of the benzyl group for the iminium substrates and the dihedrals shown by the transition structures.

If the benzyl group were to be a small substituent, it would not only need to rotate away from the chiral catalyst but also need to avoid the incoming nucleophile, even for small nucleophiles such as HCN. This issue arises for TS-6Z-S and TS-6E-R', in which the dihedral angle corresponds to a minimum on the potential energy surface of the substrate, but shows a less stable conformation in the transition state. For TS-5E-R, the dihedral angle destabilizes the transition state by about 1.8 kcal/mol, and there is an additional destabilization (about 4.1 kcal/mol) due to its interaction with the cyanide in the transition state.

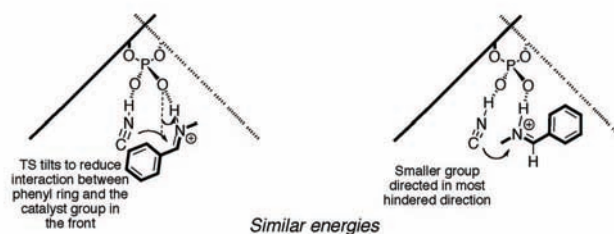
For the *E* transition states TS-5-E-S and TS-5-E-R' (Figure 7a), the imine hydrogen is outside the catalyst cavity, and both bulky groups are placed in close contact to the catalyst. Both experiments and calculations show that the benzyl group has a strong preference for the least sterically demanding position, but it is not obvious why this should be because the two sides of the imine are rather similar.

To help to understand this effect, the analogous transition states were calculated for N-methyl imines of benzaldehyde (Figure 7b). In the TS-5-E-S analogue, the steric interactions with the bulky phenyl group force the imine to tilt with respect to the phosphoric acid, and the resulting structure is slightly more stable (0.3 kcal/mol) than TS-5-E-R' analogue (Figure 7b). The geometry distortion is similar to that observed for TS-6-Z-S, but in that case the acetophenone is forced toward the other phenanthrene ring, explaining why the undistorted structure was 0.9 kcal/mol more stable. The additional destabilization of TS-5-E-R' for the N-benzyl-imine over the N-methyl-imine is a consequence of steric interactions of the benzyl ring with the catalyst phenanthrene rings. In the case of TS-5-E-S, these interactions are not present because the benzyl ring is directed away from and placed parallel to the nearer phenanthrene ring (Figure 7a). This might also explain why the best results are obtained with phenanthrene-substituted catalyst,<sup>32</sup> when smaller substituents are used (such as phenyl, 1-naphthyl or 4-biphenyl groups), TS-5-ER'-like transition structures are not so destabi-

a) Benzaldehyde-based N-benzyl imine: *E* geometry preferred in transition state



b) Benzaldehyde-based N-methyl imine: *E* geometry preferred in transition state



c) Acetophenone-based imine: *Z* geometry preferred in transition state

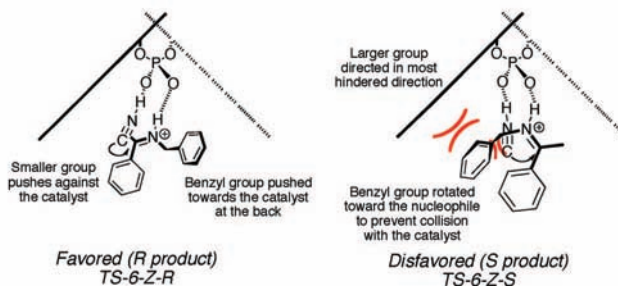


**Figure 7.** Steric interactions between the catalyst and the Strecker reaction transition states (a) benzaldehyde-derived with *E* conformation for N-benzyl imines, (b) acetophenone-derived with *Z* conformation, and (c) benzaldehyde-derived with *E* conformation for N-methyl imines.

lized since the steric interactions with the benzyl ring are less important. In addition, when big, nonplanar groups (such as 3,5-( $C_6H_5$ ) $_2C_6H_3$  or 3,5-( $CF_3$ ) $_2C_6H_3$ ) are included in the catalyst, TS-5-E-S-like transition structures are not able to accommodate the benzyl ring in a geometry in which these interactions are absent.

For the *Z* transition states, the model proposed for the selectivity in the Hantzsch ester hydrogenation of imines (Figure 1) is still applicable, provided that the benzyl group is treated as the larger group and so point in the least sterically demanding direction. The most stable TS-6-Z-R places the acetophenone methyl group close to the catalyst phenanthrene ring (Figure 7c), whereas in TS-6-Z-S the benzyl group is occupying this position. In this latter structure the imine is tilted with respect to the phosphate group in order to avoid a bad steric interaction, and this forces the benzyl group toward the other phenanthrene ring. Even this change in the geometry is not able wholly to alleviate the steric interactions, and the structure is 0.9 kcal/mol higher energy.

## Conclusion

Our calculations suggest that the Strecker reaction of N-benzylimines catalyzed by BINOL-phosphoric acid catalyst proceed through transition states in which the catalyst simultaneously bonds both the imine and the nucleophile. These

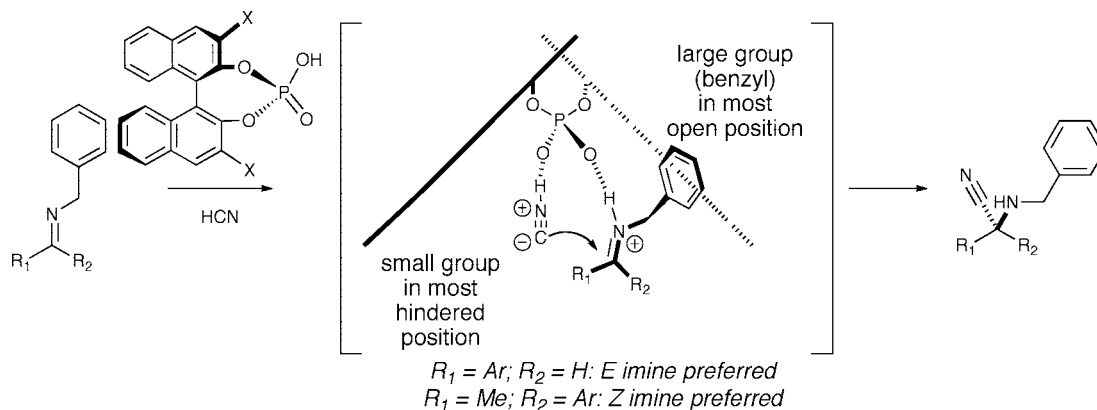


**Figure 8.** Stereochemical outcome of the BINOL–phosphoric acid-catalyzed Strecker reaction.

transition states not only show the smallest activation free energies, but also are able to reproduce the observed enantioselectivity.

These results are consistent with our earlier report of the selectivity in Hantzsch ester reductions with two differences in the transition states geometries: (i) *E*-imine geometries are preferred for benzaldehyde-derived imines; *Z*-imine geometries are preferred for acetophenone-derived imines. (ii) The benzyl group is of comparable size to an aryl group, and so is oriented in the least sterically demanding position.

The relative stability of *E/Z* transition states suggests that *p*-methoxy benzyl group might be a convenient substituent for imines derived from aldehydes for obtaining high enantioselectivity. The analysis leads to the prediction that the stereochemistry of the cyanohydrin formed from acetophenone will be opposite to that formed from benzaldehyde.

**Computational Details.** For the study of the reactions catalyzed by buta-1,3-diene-1,4-diol-phosphoric acid, calculations were performed using Jaguar program (version 6).<sup>46</sup> Geometry optimization of transition states and reactants were performed using B3LYP functional<sup>47</sup> and 6-31+G\* basis set<sup>48–50</sup> (*p*-polarization and diffuse functions were added on transferable H atoms). On these optimized structures, electronic energy was calculated using B3LYP/6-31++G\*\* level of theory and solvent (toluene) effects were introduced by means of a self-consistent reaction field procedure<sup>51,52</sup> (the dielectric constant for the solvent was 2.379 and the probe radius 2.76 Å). Gibbs free energy was calculated adding this energy to the correction to the Gibbs free energy (vibrational, rotational, and translational contributions) calculated using the same level of theory used in the optimization procedure. In addition, a correction of 1.33 kcal/mol (corresponding to  $RT \ln(V_M)$ ,  $T = 233 \text{ K}$ ,  $V_M =$  molar volume of the ideal gas at 233 K, in  $\text{dm}^3$ )

was added to correct for the Jaguar reference conditions ( $P = 1 \text{ atm}$ , 1 mol) to standard conditions ( $P = 1 \text{ atm}$ ,  $[ ] = 1 \text{ M}$ ).<sup>53</sup>

For the hybrid QM/MM calculations on real catalysts, geometry optimizations of transition structures were performed using ONIOM<sup>54–56</sup> method implemented in Gaussian03 program.<sup>57</sup> A “ball and stick” model in Figures 3 and 4 shows atoms included in the high level layer, while a wire model is used to represent atoms included in the low-level layer. A B3LYP functional<sup>47</sup> combined with 6-31G\* basis set<sup>48–50</sup> (augmented with polarization *p* functions in labile H atoms) was used in the high-level layer, and UFF molecular mechanics force field in the low-level layer.<sup>58</sup> This combination has offered excellent results in previous studies of organocatalytic mechanisms,<sup>35</sup> and the choice of the UFF force field is based on a calibration included therein. Single-point calculations on the resulting structures were performed using M05-2X functional implemented in Jaguar program (version 7),<sup>59</sup> since this functional shows good performance in reproducing organic reaction thermodynamic kinetics and nonbonding interactions.<sup>60</sup> The 6-31G\*\* basis set<sup>48–50</sup> was used for all atoms, and solvent effects (toluene, dielectric constant: 2.379; probe radius: 2.76 Å) were introduced by means of a self-consistent reaction field procedure.

For calculation of the different steric and conformational effects, atoms excluded from the study were selected in a low level layer according to a typical ONIOM<sup>54–56</sup> scheme. Gaussian03<sup>57</sup> was used to generate an external coordinate file in which the groups in the low-level layer were substituted by a H atom, according to the default treatment of interface bonds in ONIOM method<sup>54–56</sup> in Gaussian03. Single-point energy of the resulting structure was calculated with Jaguar (version 7), using the same level of theory that was employed in energy evaluation of the complete structure. The structures obtained from only those atoms included in the high-level layer atoms in Figures 3 and

(46) Jaguar, version 6.5; Schrödinger, Inc.: New York, 2006.

(47) Becke, A. D. *J. Chem. Phys.* **1983**, *98*, 5648–5652.

(48) Gill, P. M. W.; Johnson, B. G.; Pople, J. A.; Frisch, M. J. *Chem. Phys. Lett.* **1992**, *197*, 499–505.

(49) Krishnan, R.; Binkley, J. S.; Seeger, R.; Pople, J. A. *J. Chem. Phys.* **1980**, *72*, 650–654.

(50) Clark, T.; Chandrasekhar, J.; Schleyer, P. v. R. *J. Comput. Chem.* **1983**, *4*, 294–301.

(51) Tannor, D. J.; Marten, B.; Murphy, R.; Friesner, R. A.; Sitkoff, D.; Nicholls, A.; Ringnalda, M.; Goddard, W. A.; Honig, B. *J. Am. Chem. Soc.* **1994**, *116*, 11875–11882.

(52) Truhlar, D. G.; Cramer, C. J. *J. Comp. Aid. Mol. Design* **1992**, *6*, 629–666.

(53) McQuarrie, D. A. *Statistical Mechanics*; Harper and Row: New York, 1976.

(54) Svensson, M.; Humbel, S.; Morokuma, K. *J. Chem. Phys.* **1996**, *105*, 3654–3661.

(55) Vreven, T.; Morokuma, K. *J. Comput. Chem.* **2000**, *21*, 1419–1432.

(56) Dapprich, S.; Komaromi, I.; Byun, K. S.; Morokuma, K.; Frisch, M. J. *J. Mol. Struct. (Theochem)* **1999**, 461–462.

(57) Frisch, M. J.; et al. *Gaussian 03, revision D.03*; Gaussian, Inc.: Wallingford CT, 2004.

(58) Rappé, A. K.; Casewit, C. J.; Colwell, K. S.; Goddard, W. A., III; Skid, W. M. *J. Am. Chem. Soc.* **1992**, *114*, 10024–10035.

(59) Jaguar, version 7.0; Schrödinger, LLC: New York, 2007.

(60) Zhao, Y.; Schultz, N. E.; Truhlar, D. G. *J. Chem. Theory Comput.* **2006**, *2*, 364–382.

4 are not influenced by steric effects, and therefore, the relative energies calculated include only the contribution of the different substrate conformation to the relative stabilities of the transition states. When only one of the phenanthrene rings is removed, the calculated energy includes the contribution from steric effects from the remaining phenanthryl group and, again, the effect of the substrate conformation; this latter contribution, which was calculated previously, can be subtracted to estimate the steric effect of individual catalyst substituents. As expected, the summation of the steric and conformation effects yields the energy difference between the structure and the reference, within a 0.1 kcal/mol margin, which corresponds to the precision reported in the figures.

**Acknowledgment.** This research was supported by a Marie Curie Intra-European Fellowship within the 6th European Community Framework Programme MEIF-CT2006-040554. The authors acknowledge the use of CamGrid service in carrying out this work and Dr. Charlotte Bolton for IT support.

**Supporting Information Available:** Complete list of authors in the Gaussian03 reference; Cartesian coordinates of optimized structures. This material is available free of charge via the Internet at <http://pubs.acs.org>.

JA808715J